I&EC research
Industrial & Engineering Chemistry Research

pubs.acs.org/IECR
Article

Sustainable Hydrogen Production via Sorption Enhanced Reforming of Complex Biorefinery Side Streams in a Fixed Bed Adiabatic Reactor

Abdelrahman Mostafa, Irene Rapone, Aldo Bosetti, Matteo C. Romano, Alessandra Beretta,* and Gianpiero Groppi*

Cite This: *Ind. Eng. Chem. Res.* 2023, 62, 15884−15896
Read Online

ABSTRACT: In this work, sorption enhanced steam reforming is explored as a potential solution for the valorization of gaseous streams recovered from biorefinery hydrogenation processes. The hydrogen content of such streams limits the hydrocarbon conversion in conventional steam reforming due to thermodynamic and kinetic constraints. A previously developed 1D dynamic heterogeneous model of an adiabatic reactor was thus applied to evaluate the effect of H_2 dilution on the performance indicators of the sorption enhanced reforming process. The mathematical model analysis highlights that despite of CO_2 capture by the sorbent favorably modifies the thermodynamics of syngas production, H_2 dilution worsens the performance of the sorption enhanced reforming of model H_2/CH_4 streams with respect to pure CH_4. Results show a drop of 17% for CH_4 conversion and a reduction of 15.4% of the captured CO_2 on passing from pure methane to a H_2/CH_4 feed with a 40/60 molar ratio. However, on increasing the heat capacity of the bed, by replacing part of the sorbent with an inert heat carrier, better performances are calculated for the H_2/CH_4 feed matching the pure CH_4 case. The presence of C2+ hydrocarbons is assessed as well and the results show a significant improvement in the reformer's performance; in the case of a stream composed of $H_2/CH_4/C_3H_8$ with a molar ratio 40/45/15, the total hydrocarbon conversion grows to 92.8%, CO_2 capture ratio to 82.6%, and H_2 purity to 95.6%. The positive effect is associated with thermal factors that promote the reaction kinetics. Thus, the suitability of the sorption enhanced reforming technology to H_2-rich and C-poor streams is strictly composition dependent; by cofeeding of C2+ hydrocarbons, the process turns into a remarkable solution for converting gaseous streams in pure H_2.

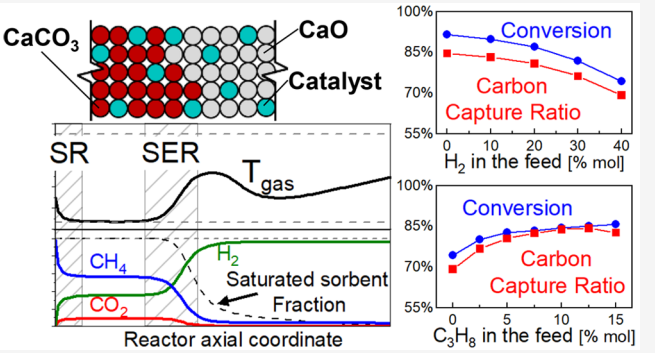

INTRODUCTION

The expected growing demand for carbon neutral fuels in the coming years[1−3] induces the development of many hydro processing technologies that focus on the production of biofuels utilizing biobased carbon neutral resources.[4−7] Thus, the need for sustainable hydrogen streams is expected to grow dramatically, as many of the fuel upgrading processes are characterized by significantly high hydrogen need. Likewise, within the conventional refinery, maximizing the hydrogen utilization, thus the refinery efficiency, along with the anthropogenic CO_2 capture are targets of the utmost importance to meet the ever-tightening emissions regulations.[8−10] Therefore, there is great interest in developing new processes for the production of sustainable carbon neutral hydrogen.[11] A novel idea is using the waste streams and the byproducts of the biorefinery to produce streams that are rich in hydrogen,[12,13] providing, besides the main benefit of covering the hydrogen demand of the biorefinery, the valorization of the biorefinery byproducts and waste streams, thus leading to reduction of the final biofuel production cost.[14] Specifically, gaseous streams separated in fractionation units downstream from hydrocracking and hydrotreating processes represent a good candidate for this application as they contain significant quantities of hydrocarbons.[15−18] However, the complex nature of such streams where they may consist of a wide range of components and could contain significant amounts of hydrogen has a severe impact on the reforming process by limiting the fuel conversion both thermodynamically and kinetically. Likewise, within the conventional refinery, hydrogenation, hydrotreating, and hydrocracking processes

Received: July 14, 2023
Revised: September 11, 2023
Accepted: September 11, 2023
Published: September 26, 2023

Table 1. Model Equations, Boundary Conditions, and Initial Conditions

Gas Phase

Overall material balance

$$\frac{\varepsilon}{u}\frac{\partial G}{\partial t} = -\frac{\partial (G)}{\partial z} + a_{v,sorbent}\sum_{i}^{NC} MW_i k_{m,i}(C_{sorbent,i} - C_{gas,i}) + a_{v,catalyst}\sum_{i}^{NC} MW_i k_{m,i}(C_{catalyst,i} - C_{gas,i})$$

i-species material balance; where i = CH_4, C_3H_8, H_2O, H_2, CO, CO_2

$$\varepsilon\frac{\partial C_{gas,i}}{\partial t} = -\frac{\partial (uC_{gas,i})}{\partial z} + D_{ae,i}\frac{\partial^2 (uC_{gas,i})}{\partial z^2} + a_{v,catalyst}k_{m,i}(C_{catalyst,i} - C_{gas,i}) + a_{v,sorbent}k_{m,i}(C_{sorbent,i} - C_{gas,i})$$

Energy balance

$$\varepsilon\rho_g cp_g\frac{\partial T_{gas}}{\partial t} = -u\rho_g cp_g\frac{\partial T}{\partial z} + \lambda_{ax}\frac{\partial^2 T}{\partial z^2} + a_{v,catalyst}h_{gs}(T_{catalyst} - T_{gas}) + a_{v,sorbent}h_{gs}(T_{sorbent} - T_{gas})$$

Momentum balance

$$\frac{\mathrm{d}P}{\mathrm{d}z} = \frac{150\mu_g(1-\varepsilon)^2}{d_p^2\varepsilon^3}u + \frac{1.75(1-\varepsilon)}{d_p\varepsilon^3}\rho_g u^2$$

Solid Phases

Catalyst material balance

$$a_{v,catalyst}k_{m,i}(C_{gas,i} - C_{catalyst,i}) = \eta(1-\varepsilon)\rho_{cat}\Sigma v_{ij}R_j$$

Sorbent material balance

$$a_{v,sorbent}k_{m,i}(C_{gas,i} - C_{sorbent,i}) = \eta(1-\varepsilon)\rho_{CaO}\Sigma v_{icarb}R_{carb}$$

$$\frac{\mathrm{d}X_{sorbent}}{\mathrm{d}t} = MW_{CaO}R_{carb}$$

Catalyst energy balance

$$(1-\varepsilon)\rho_{catalyst}cp_{catalyst}\frac{\partial T_{catalyst}}{\partial t} = a_{v,catalyst}h_{gs}(T_{gas} - T_{catalyst}) - (1-\varepsilon)\rho_{catalyst}\Sigma\eta R_j\Delta H_{R,j}$$

Sorbent energy balance

$$(1-\varepsilon)\rho_{sorbent}cp_{sorbent}\frac{\partial T_{sorbent}}{\partial t} = a_{v,sorbent}h_{gs}(T_{gas} - T_{sorbent}) - (1-\varepsilon)\rho_{CaO}R_{carb}\Delta H_{carb}$$

Boundary Conditions

Reactor inlet ($z = 0$)

$$F_{gas,tot} = C^0_{gast,tot}v^0_{gas}$$

$$C^0_{gas,i} = C_{gas,i} - \frac{D_{ae,i}\partial C_{gas,i}}{v_{gas}\partial z}$$

$$T^0_{gas} = T_{gas} - \frac{\lambda_{ax}\partial T_{gas}}{v_{gas}Cp_{gas}\partial z}$$

Reactor outlet ($z = L_t$)

$$\frac{\partial C_{gas,i}}{\partial z} = 0$$

$$\frac{\partial T_{gas}}{\partial z} = 0$$

Initial Conditions

For all the reactor length ($0 < z < L_t$)

$T_{gas} = T_{catalyst} = T_{sorbent} = T_{(solids\text{-}initial)}$

$C_{gas,i} = C^{t=0}_{gas,i}$

$X_{sorbent} = 0$

take place in the presence of excess H_2 to produce, besides the main products, gaseous streams containing high concentration of H_2.[19] Combining the chemical reactions and product separation in a single step makes the sorption enhanced reforming (SER) a very promising option for achieving a high hydrogen yield from such complex streams.

In the SER process, the continuous CO_2 removal through the carbonation of metal oxides (eq 1) shifts the thermodynamic equilibrium of the hydrocarbons steam reforming (SR) reaction (eq 2) and the water gas shift (WGS) reaction (eq 3) toward the production of H_2 according to the Le Chatelier's principle, improving the hydrogen yield and purity.[20,21] The integration of H_2 production and purification in a single step intensifies the process and in practice eliminates the need of downstream separation stages. Additionally, the SER process couples the endothermic hydrogen production, via reforming reactions, with exothermic carbon dioxide adsorption which reduces the energy demand in the reforming step of the process, alleviating the need for direct fuel combustion.

$$\mathrm{MeO} + \mathrm{CO_2} \leftrightarrow \mathrm{MeCO_3} \quad \Delta H_r^0 < 0 \tag{1}$$

$$\mathrm{C_nH_{2n+2}} + n\mathrm{H_2O} \leftrightarrow n\mathrm{CO} + (2n+1)\mathrm{H_2} \quad \Delta H_r^0 > 0 \tag{2}$$

$$\mathrm{CO} + \mathrm{H_2O} \leftrightarrow \mathrm{CO_2} + \mathrm{H_2} \quad \Delta H_r^0 = -41\ \mathrm{kJ\ mol^{-1}} \tag{3}$$

A key element for a successful SER process is the appropriate selection of high-temperature sorbents. The choice of suitable sorbents for selective in situ CO_2 removal from the reaction medium is a great challenge due to the severe

https://doi.org/10.1021/acs.iecr.3c02401
Ind. Eng. Chem. Res. 2023, 62, 15884−15896

operating conditions, especially the high temperature and the presence of steam during the sorption process.[22] Many promising materials have been tested and developed as potential sorbents, including CaO-based, hydrotalcite-based, and alkaline ceramic sorbents[23,24] among which CaO-based solids are the most attractive due to their wide availability, low cost, high theoretical sorption capacity and fast carbonation kinetics.[25]

Besides the several experimental and modeling studies performed on the SER of methane,[26−29] some studies have also considered the use of biomass sources as feedstock, such as ethanol,[30,31] glucose,[32] glycerol,[33,34] bio-oil,[12−14] and more recently biogas.[35] The proven feasibility of utilization of the SER process with a wide range of feed streams makes it an ideal candidate for selective hydrogen production from complex streams. In this respect, the goal of this work is the evaluation of the suitability of integrating the sorption enhanced reforming process within a refinery/biorefinery scheme utilizing model mixtures representative of some side streams of the refinery to produce pure streams of hydrogen to be used internally in the fuel upgrading processes or to be exported.

In our recent work,[36] a 1D heterogeneous model for the methane SER process in an adiabatic fixed bed reactor was developed. The model allowed for a detailed analysis of the dynamic behavior of the process under the adiabatic conditions, highlighting the importance of the bed thermal capacity on the methane conversion and the carbon capture ratio (CCR). The effects of the inlet gas, the initial solid temperatures, and of inert heat carrier addition were investigated. Simulation results for pure methane streams showed that CH_4 conversion and H_2 yield in excess of 90% could be obtained together with an H_2 purity >95% and an 85% CCR. Besides, the possibility to operate the SER process with a high initial solid temperature was highlighted, which minimizes the need of a cooling step between sorbent regeneration and reforming stages with beneficial implications on the overall efficiency of the process. In this work, we extend the model analysis of the sorption enhanced reforming process in the adiabatic fixed bed arrangement utilizing a range of mixed streams, mainly rich in hydrogen, representative of the gaseous side streams available in refineries and industrial plants. The effect of the hydrogen presence in such streams is discussed by performing several simulations using the 1D model. Then, the presence of C2+ hydrocarbons in the feeding mixture of the SER process is assessed.

METHODOLOGY

SER Reactor Model. In our previous work,[36] a heterogeneous 1D dynamic model of a fixed bed reactor was developed. The model describes the dynamic evolution of concentration and temperature axial profiles across the SER reactor by solving the dynamic differential mass and energy balances and incorporating the kinetics and thermodynamics of all chemical processes, namely, the 1D total mass balance for gas phase, 1D *i*-species mass balance (i = CH_4, H_2O, H_2, CO, CO_2, N_2, C_3H_8), and energy balances for the gas phase, catalyst, and sorbent solid phases are included in the model. The internal diffusion limitations in the catalyst particles are accounted by including a global catalyst effectiveness factor in the *i*-species mass balance similar to works presented in the literature.[37−41] The model equations, along with the boundary and initial conditions, are presented in Table 1 (see Supporting Information for Nomenclature). Due to the very low Biot number calculated at the selected working conditions, particles are assumed to be isothermal. The modeled reactor scheme and dimensions are reported in section A of the Supporting Information. The model is implemented in gPROMS software platform for the dynamic simulation following the same numerical scheme detailed in our previous work.[36]

Four catalytic reactions are considered in this work, methane reforming, propane reforming, methanation, and water gas shift, combining the C1 kinetic model developed by Xu and Froment[42] for nickel catalyst with the propane steam reforming model reported by Uskov et al.[43] Regarding the kinetic model used for the CaO carbonation, due to the insignificant contribution of the slow diffusion controlled step in any practical CO_2 capture application as described by Mess et al.,[44] the empirical rate equation presented in[45] with a rate constant invariant with temperature and a constant maximum sorbent conversion is used as discussed in ref 36. All the rate equations and the kinetic and equilibrium parameters for both the catalytic and the sorption reactions are reported in sections B and C of the Supporting Information. The reactions' enthalpies are calculated for the various catalyst and sorbent phases temperatures using the correlations and the coefficients for calculating the specific heat capacities and the enthalpies of formation of all the species from.[46] gPROMS Multiflash 4.3 utility tool is used to calculate the physical and chemical properties (molecular weight, specific heat, density, viscosity, and thermal conductivity) of the reacting mixture. Molecular diffusivities, mass, and heat transport coefficients are calculated with correlations taken from the literature[47−51] and reported in section D of the Supporting Information.

RESULTS AND DISCUSSION

Dynamic Behavior of H_2-Rich Stream SER in a Fixed Bed Reactor. A typical arrangement of the SER process in a fixed bed can approach a continuous production of hydrogen through alternating parallel reactors between the two steps of the process: the sorption enhanced reforming and the sorbent regeneration. Using the 1D heterogeneous model described in section 2, the performance of the sorption enhanced reforming of hydrogen containing streams is evaluated in an adiabatic fixed bed reactor (2.26 m diameter and 5 m length). On the basis of our previous modeling work,[36] baseline working conditions are selected to perform the process at a pressure of 10 bar with a steam to carbon ratio of 4, a feeding temperature of 550 °C and an initial bed temperature of 850 °C. The simulations were performed assuming a GHSV = 350 N $m^3/h/m^3_{reactor}$ and that the reactor is packed with spherical sorbent and catalyst particles of 2 mm diameter at a sorbent to catalyst ratio of 5 v/v. Table 2 summarizes the geometric and operating parameters used in the simulations. It is worth mentioning that a summary of the operating conditions used for all the simulations herein discussed is reported in section E of the Supporting Information.

Limited by the amount of the loaded active sorbent in the reactor, SER is a dynamic process in the fixed bed arrangement as demonstrated in ref 52. In our previous work,[36] a detailed description of the dynamic behavior of the methane sorption enhanced reforming process is carried out in an adiabatic fixed bed reactor. As shown in Figure 1, schematizing the reactor's axial profiles of temperature and composition at any time step before the breakthrough, the introduction of the feeding mixture to the reactor initiates the globally endothermic

https://doi.org/10.1021/acs.iecr.3c02401
Ind. Eng. Chem. Res. 2023, 62, 15884−15896

Table 2. Reactor Characteristics and Operating Conditions for the Reference Case

feed gas temperature	550	°C
initial solids temperature	850	°C
pressure	10	bar
steam to carbon molar ratio	4	mol/mol
sorbent to catalyst ratio	5	m^3_{CaO}/m^3_{Cat}
catalyst particle density	1650	kg/m^3
sorbent particle density	1650	kg/m^3
reactor diameter	2.26	m
reactor length	5	m
particle diameter ($d_{particle}$)	2	mm
GHSV	350	N $m^3/h/m^3_{reactor}$
max sorbent conversion (X_{max})	0.4	mol_{caco3}/mol_{cao}
catalyst effectiveness factor (η)	0.3	
void fraction (ε)[a]	0.4	

[a]Calculated according to eq S1 in section A of the Supporting Information.

reactions taking place on the catalyst surface in the reactor inlet zone, resulting in a drop in the temperature of the solid phase and producing CO_2 in the gas phase. Along with the reformate, the CO_2 migrates downstream the bed until reaching the front of the fresh sorbent zone that rapidly consumes most of the CO_2 in the gas phase, shifting reaction equilibria and resulting in a locally exothermic process, which generates significant temperature and composition gradients. The exothermic SER produces a high temperature wave that advances through the bed, controlled by two factors: the convective heat transfer by the gas phase and the incremental saturation of the sorbent leading to the forward movement of the SER zone. This latter effect makes the peak of the thermal wave progressively higher, while the convective heat transfer, which propagates faster than the SER front, makes it progressively wider. Eventually, the moving carbonation front reaches the outlet of the reactor, turning the behavior of the reactor to that of an equilibrated adiabatic steam reformer. This complex framework justifies the temporal temperature and composition profiles at the reactor outlet plotted in Figure 2.

Focusing on the simulation results for the pure methane case represented with the red line in Figure 2, the temperature and composition of the stream exiting the reactor pass by four temporal phases. Initially, there is a period characterized by steady conditions (constant temperature and composition) of the stream exiting the reactor, whose duration is controlled by the heat capacity of the reactor bed. Then, as a result of the progressive cooling of the reactor bed due to relatively low inlet gas temperature and the endothermic nature of the SER global reaction, the reactor enters in the thermal breakthrough phase, when the outlet temperature presents a complex evolution, first decreasing and then increasing again, although to a limited extent. Such a reduction of the outlet temperature limits the extent of methane conversion, but the availability of active sorbent still removes the CO_2 produced by the WGS reaction, maintaining high hydrogen purity in the outlet stream. Notably, the complex evolution of the outlet temperature during the thermal breakthrough phase is associated with the propagation of the SER thermal wave described above. As the sorbent in the reactor becomes saturated the material breakthrough phase, characterized by a steep increase of CO_2 concentration in the outlet stream, takes place. Finally, the complete saturation of the sorbent is reached, and the reactor evolves to the post breakthrough phase acting as a conventional methane reformer under adiabatic conditions, with quite low methane conversion and H_2 production.

Comparing the breakthrough curve for pure methane with those calculated for 20/80 (blue line) and 40/60 (green line) H_2/CH_4 feed molar ratios (Figure 2), a similar behavior is predicted since the time evolution of the outlet variables follows the same temporal phases described for the pure methane case. However, during the thermal breakthrough phase, lower average outlet temperatures are calculated (from 648 °C in the case of pure CH_4 SER to 604 °C in the case of H_2/CH_4 = 40/60 feed molar ratio), resulting in lower CH_4 conversion (panel B) during the thermal breakthrough phase (dropping from 87.5% to 67.6%) on increasing the H_2 content in the feed. As explained in ref 36 and summarized above, the complex temperature dynamics in the thermal breakthrough phase is governed by the combination of the cooling effect of the cold inlet gas and the endothermic steam reforming process, which occurs at the very inlet of the catalyst bed, with the heating effect of exothermic process in the carbonation zone. The two effects propagate through the bed with different velocities, resulting in the initial temperature decline followed by a temperature increase occurring in the thermal breakthrough phase, where the SER zone reaches the outlet section of the reactor.

As shown in Figure 3A–C, where axial temperature and concentration profiles at a single time step before the breakthrough are reported, the presence of H_2 in the feed (solid lines) limits the conversion of methane in the steam

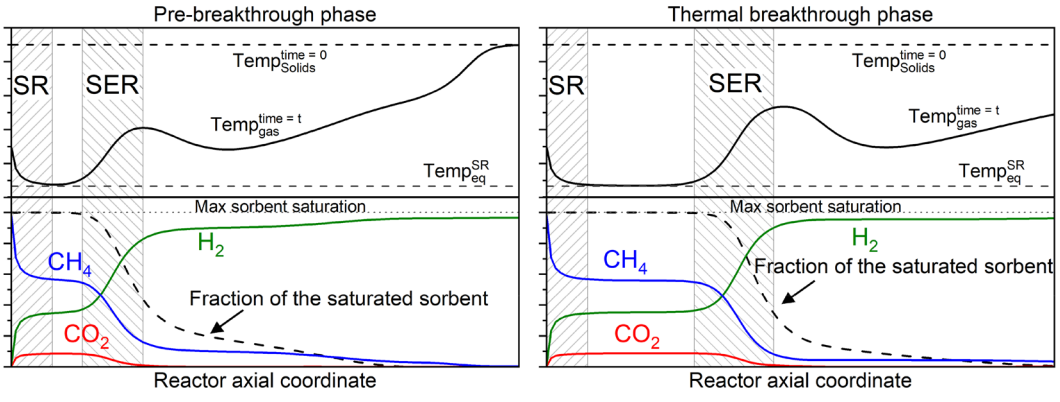

Figure 1. Temperature and composition development along the axis of the reactor.

https://doi.org/10.1021/acs.iecr.3c02401
Ind. Eng. Chem. Res. 2023, 62, 15884−15896

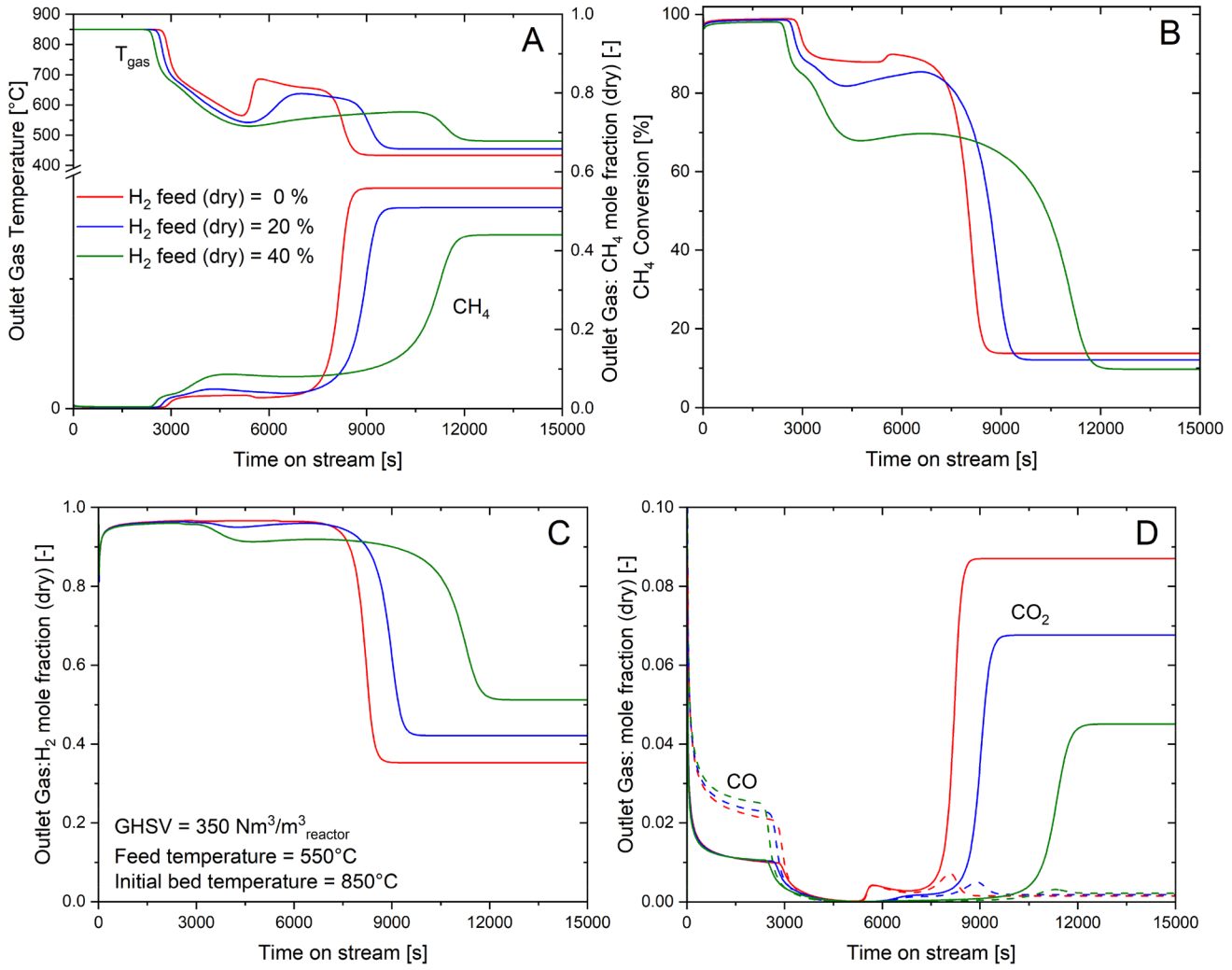

Figure 2. Effect of the H_2 content in the feed on the breakthrough curves. P = 10 bar; S/C = 4; T_{feed} = 550 °C; $T_{bed,initial}$ = 850 °C; GHSV = 350 N $m^3/m^3_{reactor}$.

reforming zone (where the sorbent is already saturated) at the reactor entrance, resulting in lower CO_2 concentrations compared to the pure CH_4 feed (dashed lines). Since the extent of steam reforming in the entry zone is responsible for the exothermicity of the process in the SER zone, which is mainly due to the excess of carbonation rate compared with the reforming rate (Figure 3d), H_2 dilution also mitigates the local heat release in the SER zone. Such effects smooth the thermal wave associated with SER and result in a less pronounced temperature increase in the ending part of the thermal breakthrough phase. The lower extent of CH_4 conversion combined with the slightly lower feed carbon concentration also results in an evident delay of the material breakthrough time on increasing H_2 feed content (Figure 2).

The integral performances of the SER reaction step are evaluated based on the set of key performance indices (KPIs) calculated with eqs 4−8 by integrating the molar flow rates inlet and outlet over the breakthrough time (BTt); this was selected as the time required to reach an outlet CO_2 molar fraction of 0.02 on dry basis.

Integral CH_4 conversion

$$= \frac{\int_0^{BTt} \dot{n}\mathrm{CH}_4^{in}\,\mathrm{d}t - \int_0^{BTt} \dot{n}\mathrm{CH}_4^{out}\,\mathrm{d}t}{\int_0^{BTt} \dot{n}\mathrm{CH}_4^{in}\,\mathrm{d}t} \quad (4)$$

Integral net hydrogen yield

$$= \frac{\int_0^{BTt} \dot{n}\mathrm{H}_2^{out}\,\mathrm{d}t - \int_0^{BTt} \dot{n}\mathrm{H}_2^{in}\,\mathrm{d}t}{4\int_0^{BTt} \dot{n}\mathrm{CH}_4^{in}\,\mathrm{d}t} \quad (5)$$

Integral hydrogen purity

$$= \frac{\int_0^{BTt} \dot{n}\mathrm{H}_2^{out}\,\mathrm{d}t}{\int_0^{BTt} \dot{n}\,\mathrm{total}^{out}\,\mathrm{d}t - \int_0^{BTt} \dot{n}\mathrm{H}_2\mathrm{O}^{out}\,\mathrm{d}t} \quad (6)$$

Integral carbon capture ratio (CCR)

$$= \frac{\int_0^{BTt} NC_i\dot{n}_i^{gas\text{-}in}\,\mathrm{d}t - \int_0^{BTt} NC_i\dot{n}_i^{gas\text{-}out}\,\mathrm{d}t}{\int_0^{BTt} NC_i\dot{n}_i^{gas\text{-}in}\,\mathrm{d}t} \quad (7)$$

https://doi.org/10.1021/acs.iecr.3c02401
Ind. Eng. Chem. Res. 2023, 62, 15884−15896

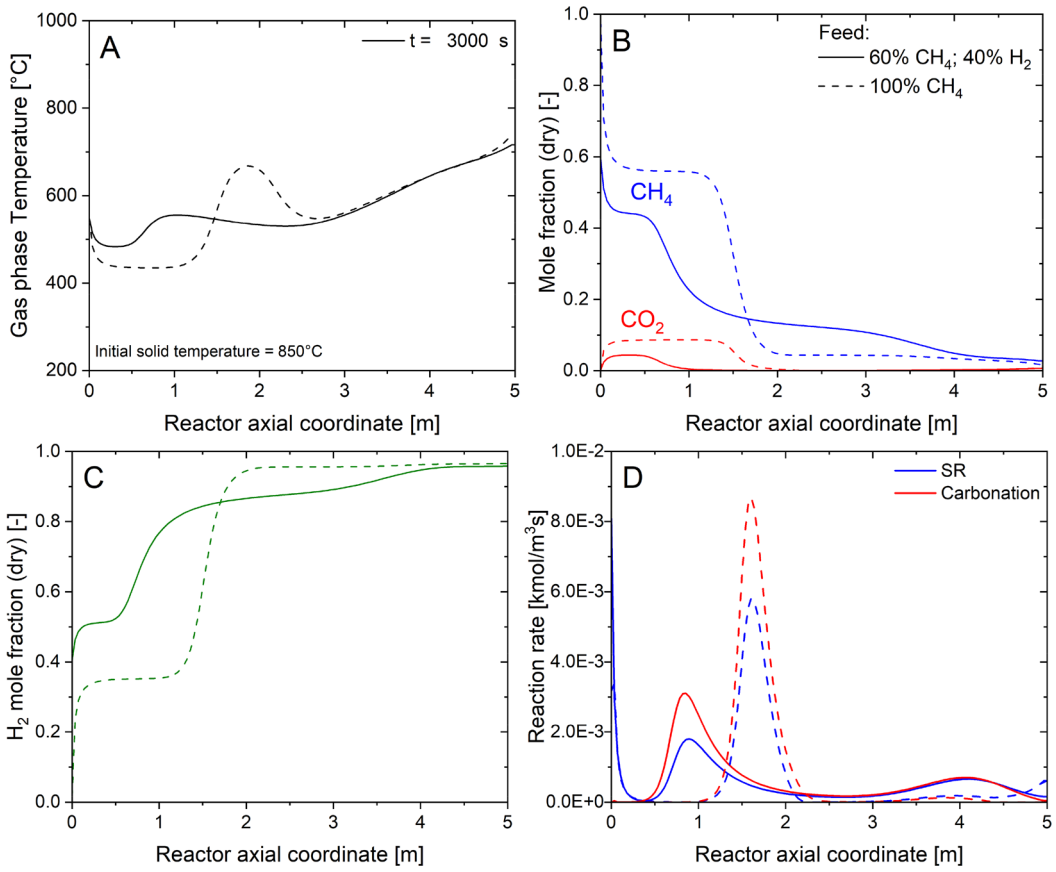

Figure 3. Axial profiles of temperature, concentration, and rates of reaction at t = 3000s. Solid lines: pure CH_4 feed; dashed lines: H_2/CH_4 = 40/60 feed molar ratio.

$$\text{Sorbent bed utilization} = \frac{\int_0^L n_{CaCO_3}(BTt)\,dz}{\int_0^L n_{CaO}(t=0)\,dz} \quad (8)$$

As presented in Figure 4, the increased content of hydrogen in the feed hinders the methane reforming, reducing the efficiency of the hydrogen production process. The conversion drops from 91.5% to 74.4% on passing from a feed stream of pure CH_4 to a stream containing 40/60 mol/mol H_2/CH_4. Following the decline of conversion, the carbon capture ratio decreased from 84.6% to 69.2%, with unconverted methane as the main carbon species at the reactor outlet. However, the increased outlet methane concentration has a lower effect on the H_2 purity, with just 3.8% reduction from 95.9% to 92.1%, due to the presence of H_2 in the feed stream. Reduced methane conversion is responsible for the reduction of the net H_2 yield from 89.5% to 73%.

Given the significant drop in performance, a sensitivity analysis to evaluate the effect of the GHSV and the steam to carbon ratio on the SER of the H_2-rich stream is performed and as reported in section F of the Supporting Information, results show a limited improvement of the KPIs on decreasing the GHSV and on increasing the stream to carbon ratio.

Effect of Inert Heat Carrier Addition. As proposed in our previous work,[36] the partial replacement of sorbent with dense inert pellets (ρ_{inert} = 3950 kg/m^3 and Cp_{inert} = 0.88 kJ/kg/K) is a strategy to balance the heat and CO_2 capture capacities of the reactor. To evaluate the effectiveness of this strategy on the SER of H_2-containing stream, simulations are performed replacing 20% (ξ_{inert} = 0.16) and 40% (ξ_{inert} = 0.34) of the sorbent volume with the inert material, keeping fixed the catalyst volume fraction of the reference case with no inert addition. In line with the results achieved for the pure methane SER,[36] the simulated breakthrough curves presented in Figure 5 for a stream of H_2/CH_4 feed molar ratio of 40/60, show a slight elongation in the pre-break-through phase with increase of the inert solid fraction thus the growth of the bed thermal capacity. On the other hand, the material breakthrough is markedly brought forward due to the lower amount of sorbent in the bed. As a consequence, the thermal breakthrough phase becomes shorter and characterized by a significant upsurge in the simulated outlet stream temperature that grows progressively with the increase in the inert solid fraction.

Evaluating the process KPIs, as presented in Figure 6, the methane conversion improves with the inert's volumetric fraction, growing from 74.4% for the reference case with ξ_{inert} = 0 to 93.4% for the case with ξ_{inert} = 0.34. The higher conversion is coupled with a higher hydrogen yield (from 73% to 90%), higher carbon capture ratio (from 70.2% to 77.7%), and a slight growth (from 92.1% to 95%) in the H_2 purity, as well. Even though the conversion grows significantly (an increase of 19%), the elongation of the pre-break-through phase and the excessive increase of the temperature during the thermal breakthrough phase limits the WGS reaction and hinders the carbonation reaction resulting in a limited improvement of the CCR and the H_2 purity.

Notably, the simulated reduction of the breakthrough time with the inert solid fraction results in an increased number of reaction−regeneration cycles, which may lead to technical hurdles on a plant scale. Therefore, a global technoeconomic

https://doi.org/10.1021/acs.iecr.3c02401
Ind. Eng. Chem. Res. 2023, 62, 15884−15896

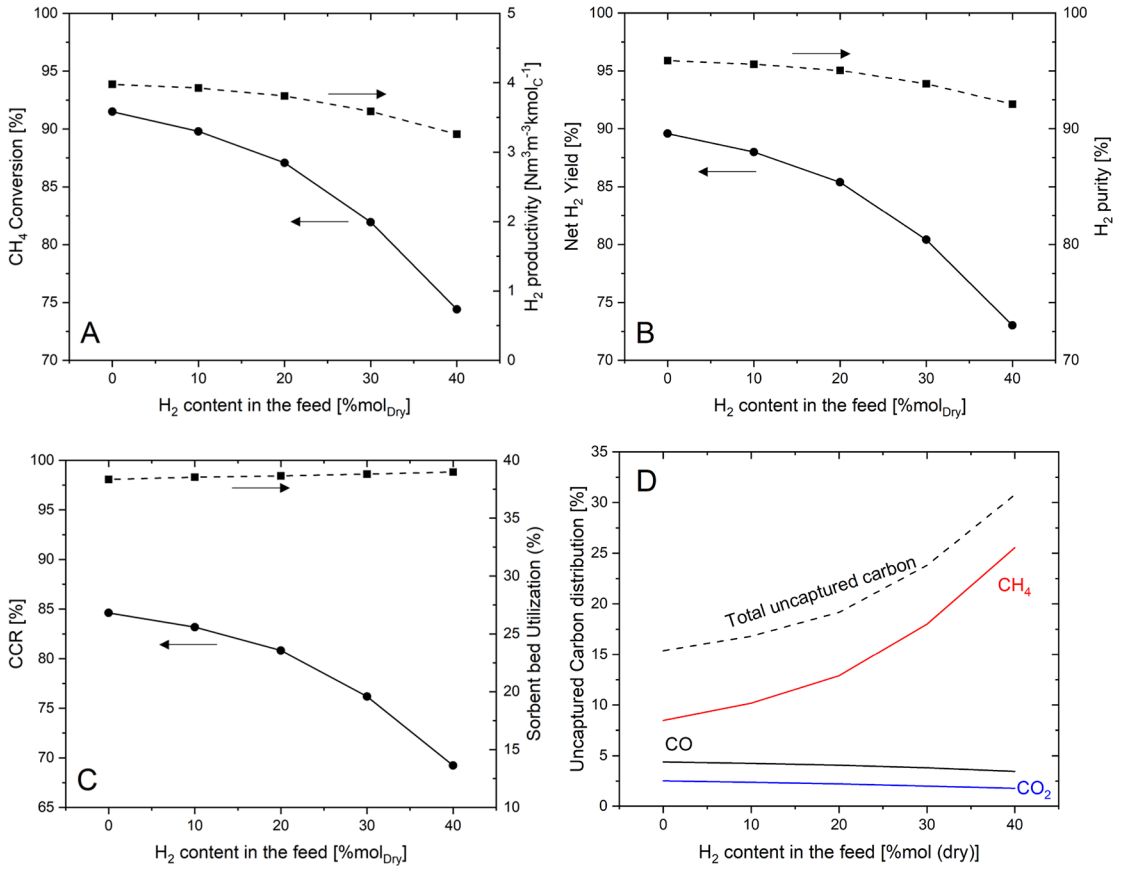

Figure 4. Effect of the hydrogen cofeed on the integral performances of the SER process.

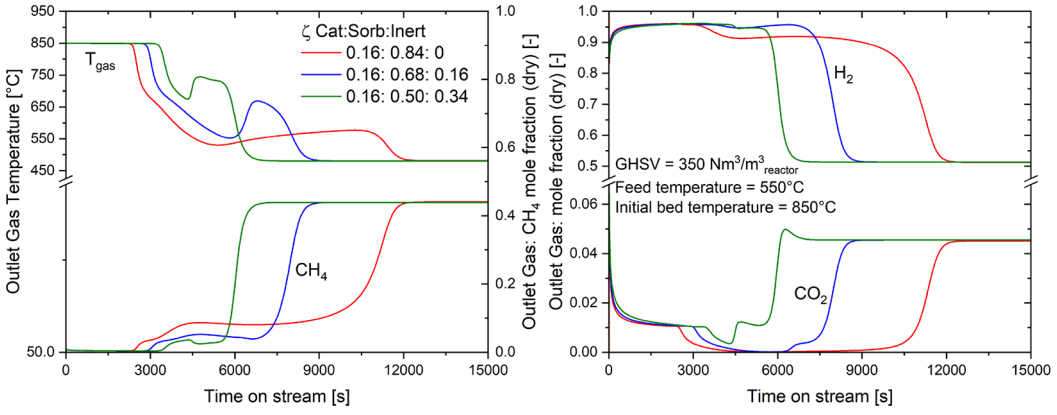

Figure 5. Effect of inert heat carrier addition on the breakthrough curves. H_2/CH_4 feed molar ratio = 40/60; P = 10 bar; S/C = 4; T_{feed} = 550 °C; $T_{bed,initial}$ = 850 °C.

analysis of the full cycle reaction-regeneration is necessary to evaluate the feasibility of addition of inert solids on the overall plant performance.

It is worth mentioning that the analysis on the impact of inert solids on the SER process is also relevant for the SER step of the Ca−Cu process, a peculiar SER process where sorbent regeneration is carried out though a Cu/CuO chemical loop.[53−55] In the SER step of the Ca−Cu process, the Cu particles behave as inert material that would affect the thermal capacity of the reactor bed, making the physical properties of the Cu containing material an important parameter for the optimization of the Ca−Cu chemical looping process.

Effect of C2+ Hydrocarbons Presence in the Feed. In the framework of the complex refinery side streams, the effect of higher hydrocarbons is particularly interesting to study. In this analysis, propane is used as a representative molecule for C2+ hydrocarbons. The effect of the presence of propane in a stream containing hydrogen is studied by assuming a stream containing 40% (dry) hydrogen and 60% (dry) hydrocarbons distributed between propane and methane. In Figure 7, the breakthrough curves obtained for different feed propane content are compared. The average outlet stream temperature in the thermal breakthrough phase markedly increases with the content of propane in the feed rising from 604 °C for the case with no propane cofeeding to 737 °C for the case with 15%

https://doi.org/10.1021/acs.iecr.3c02401
Ind. Eng. Chem. Res. 2023, 62, 15884−15896

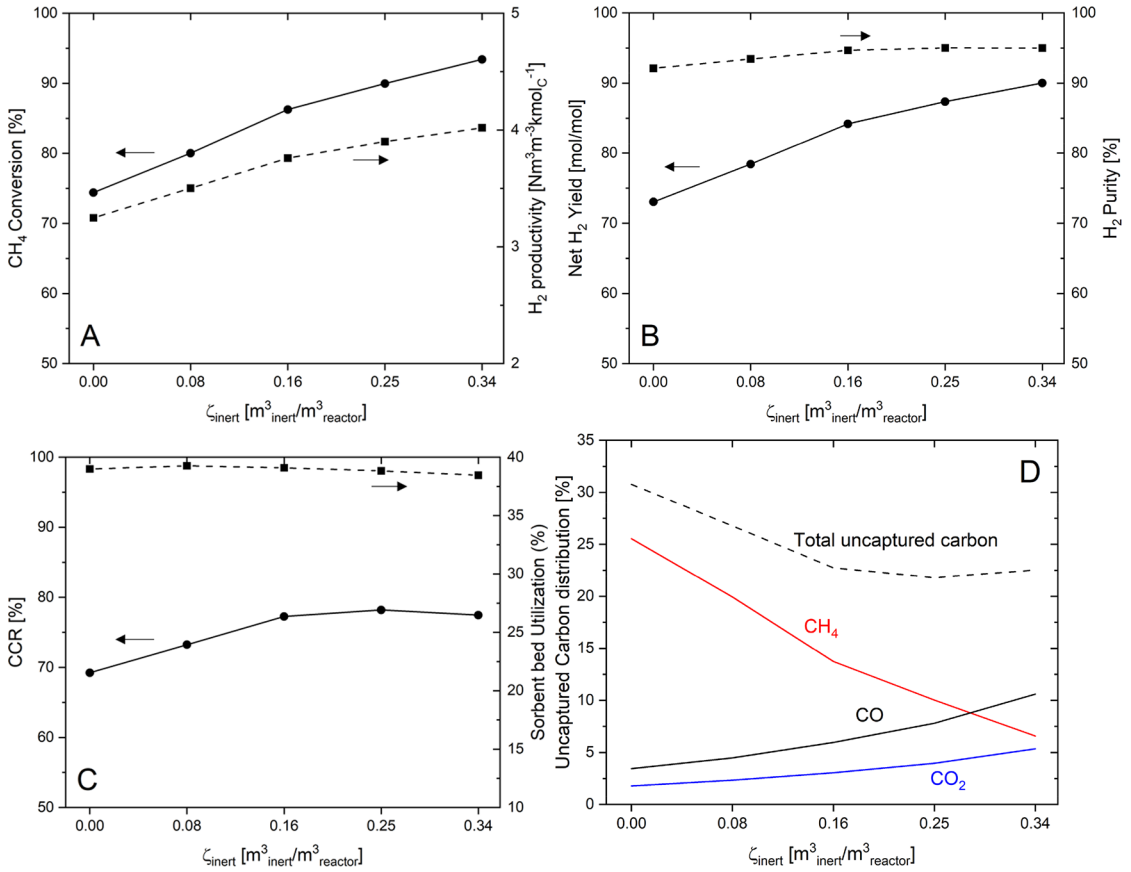

Figure 6. Effect of the inert heat carrier addition on the KPIs of the H_2-rich stream SER process.

mol (dry) C_3H_8 in the feed. Similarly, the hydrocarbon conversion (panel B) during the thermal breakthrough phase increases from 67.6% without propane to 91% with 15% mol (dry) C_3H_8 in the feed. This behavior is explained by the more favorable thermodynamics of C_3H_8 steam reforming, which allows a higher C-conversion in the SR zone where the sorbent is saturated, resulting in a more pronounced extent and lower endothermic contribution of the steam reforming reaction in the inlet zone. Accordingly, the overall exothermicity of the process in the SER zone progressively increases with the C_3H_8 feed content, resulting in a more pronounced temperature increase in the second part of the thermal breakthrough phase.

To evaluate the effect of the presence of propane in the feed on the integral scale of the process, a reassessment of the KPIs is needed. Equations 9 and 10 define the integral hydrocarbon conversion and the integral net hydrogen yield, respectively, including the presence of both methane and propane in the feed.

Integral hydrocarbons conversion

$$= \frac{\int_0^{BTt} \dot{n}CH_4^{in} + 3\dot{n}C_3H_8^{in}\,dt - \int_0^{BTt} \dot{n}CH_4^{out} + 3\dot{n}C_3H_8^{out}\,dt}{\int_0^{BTt} \dot{n}CH_4^{in} + 3\dot{n}C_3H_8^{in}\,dt} \quad (9)$$

Integral net hydrogen yield

$$= \frac{\int_0^{BTt} \dot{n}H_2^{out}\,dt - \int_0^{BTt} \dot{n}H_2^{in}\,dt}{4\int_0^{BTt} \dot{n}CH_4^{in}\,dt + 10\int_0^{BTt} \dot{n}C_3H_8^{in}\,dt} \quad (10)$$

As evident from Figure 8, the propane content in the feed markedly enhances the hydrocarbon conversion (from 74.4% without propane to 92.8% with 15% mol (dry) C_3H_8 in the feed), taking advantage from complete propane conversion calculated in all the simulations performed. Besides methane conversion also increases with the feed propane content (74.4% without C_3H_8 to 85.8% with 15% mol C_3H_8), which can be explained by the increase of the average outlet temperature as deduced from the breakthrough curves. The enhanced conversion is reflected in an increase of the net H_2 yield rising from 73% for no C_3H_8 cofeeding to 89.2% for the case with 15% mol C_3H_8 cofeeding. On the other hand, CCR exhibits a different behavior with an increasing trend from 69.2% to 84.3% on increasing the propane content from 0% to 12.5%, followed by a slight decrease to 82.6% for the case with 15% mol C_3H_8. The initial increase of the CCR at the lower range of propane cofeeding is consistent with the hydrocarbon conversion trend coupled with the moderate temperature of the reactor, maintaining high sorption performance. On the other hand, at the highest investigated concentration of propane in the feed, the increasing exothermicity of the process leads to an increase of the temperature in the moving carbonation zone, resulting in a reduction of the performance of the sorbent. This explanation is clear from the distribution of the uncaptured carbon containing species (Figure 8D), which is largely dominated by unconverted CH_4 at low feed propane concentrations, with a contribution of CO_x which becomes significant only at the highest C_3H_8 feed concentration. The specific H_2 productivity per unit mole of carbon feed and the H_2 purity follow the same trend of the CCR achieving a maximum H_2 productivity of 3.64 N m^3 $m^{-3}_{reactor}$

https://doi.org/10.1021/acs.iecr.3c02401
Ind. Eng. Chem. Res. 2023, 62, 15884−15896

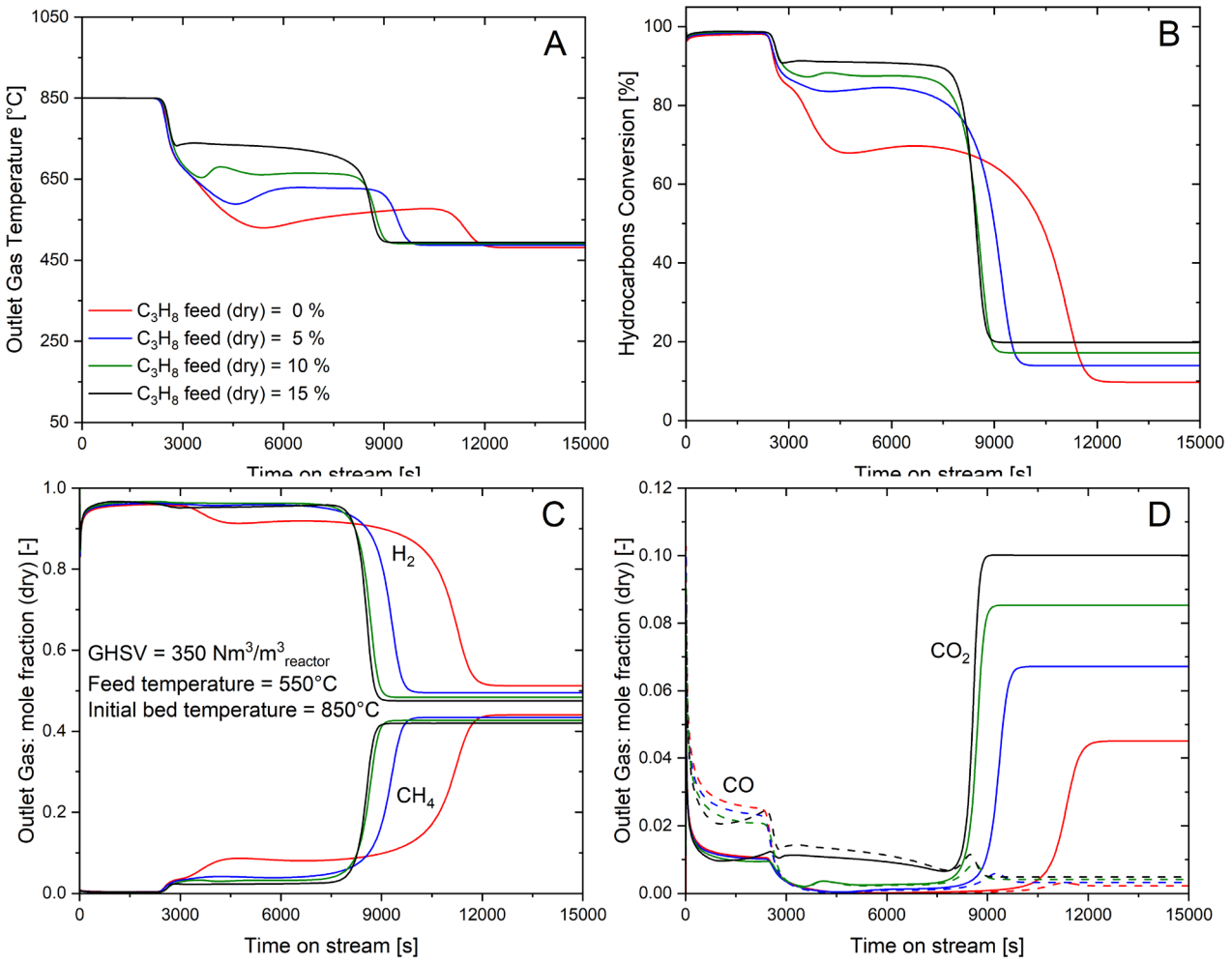

Figure 7. Effect of the presence of C2+ species on the breakthrough curves. Working conditions: P = 10 bar; S/C = 4; T_{feed} = 550 °C; $T_{bed,initial}$ = 850 °C.

$kmol_C^{-1}$ at 10% mol propane cofeeding and a maximum purity of 96% at 12.5% mol propane cofeeding.

The presented results suggest a flexibility of the SER process in terms of the feeding mixture composition, where reforming of complex streams that contain high concentration of H_2 becomes feasible by cofeeding of a small amount of C2+ hydrocarbons. Enrichment of carbon poor streams leads to matching the thermal demand of the reforming process and ensures extracting better performance from the reformer.

Assessment of a Full-Scale Fixed Bed SER Reactor. A benchmark is required to properly assess the SER performance in an adiabatic fixed bed reactor arrangement. The dynamic temperature profiles simulated in this work for the fixed bed arrangement cover a wide range from less than 500 °C (adiabatic SR temperature with T_{feed} = 550 °C) to 850 °C (initial solid temperature). In view of this, the calculated integral performance indices for the different feeding streams addressed in this work are compared with the calculated SER equilibrium values in isothermal and isobaric conditions for two reference cases: 600 and 700 °C; using the same steam to carbon ratio and pressure values used to perform the adiabatic fixed bed simulations (S/C = 4, P = 10 bar). The methods used to perform equilibrium calculation along with more detailed results are reported in section G of the Supporting Information of this work. It is noteworthy that isothermal equilibrium values are representative of the performances of interconnected circulating fluidized SER/Regeneration beds operated at uniform and constant temperatures as a result of intense solid recirculation and low solid replacement to inventory ratio.

Figure 9 presents a comparison between the KPIs resulting from model simulations of the fixed bed reactor and the values calculated for the equilibrium condition at constant temperature and pressure for three feeding mixtures: pure methane; Mix 1:40/60 H_2/CH_4 mol/mol; Mix 2:40/45/15 $H_2/CH_4/C_3H_8$ mol/mol. For Mix 1 the case with inert addition is also considered.

As shown in Figure 9A, the calculated integral hydrocarbon conversion for the simulated adiabatic fixed bed reactor outperforms the equilibrium values in all of the investigated cases except for Mix 1 without inert addition. This is due to the high outlet temperature before and, to a minor extent, during the thermal breakthrough, which enhances the hydrocarbon conversion by steam reforming. On the other hand, the calculated CRR (Figure 9C) keeps slightly below equilibrium values, consistent with the lower CO_2 capture capacity of the sorbent on increasing the temperature. The lower calculated CCR results in slightly lower H_2 purity compared to the equilibrium values, as evident in Figure 9D of the figure. It is worth emphasizing that this decrease of carbon capture performances is quite limited since most of the sorbent in the SER zone operates at lower temperature compared to the

https://doi.org/10.1021/acs.iecr.3c02401
Ind. Eng. Chem. Res. 2023, 62, 15884−15896

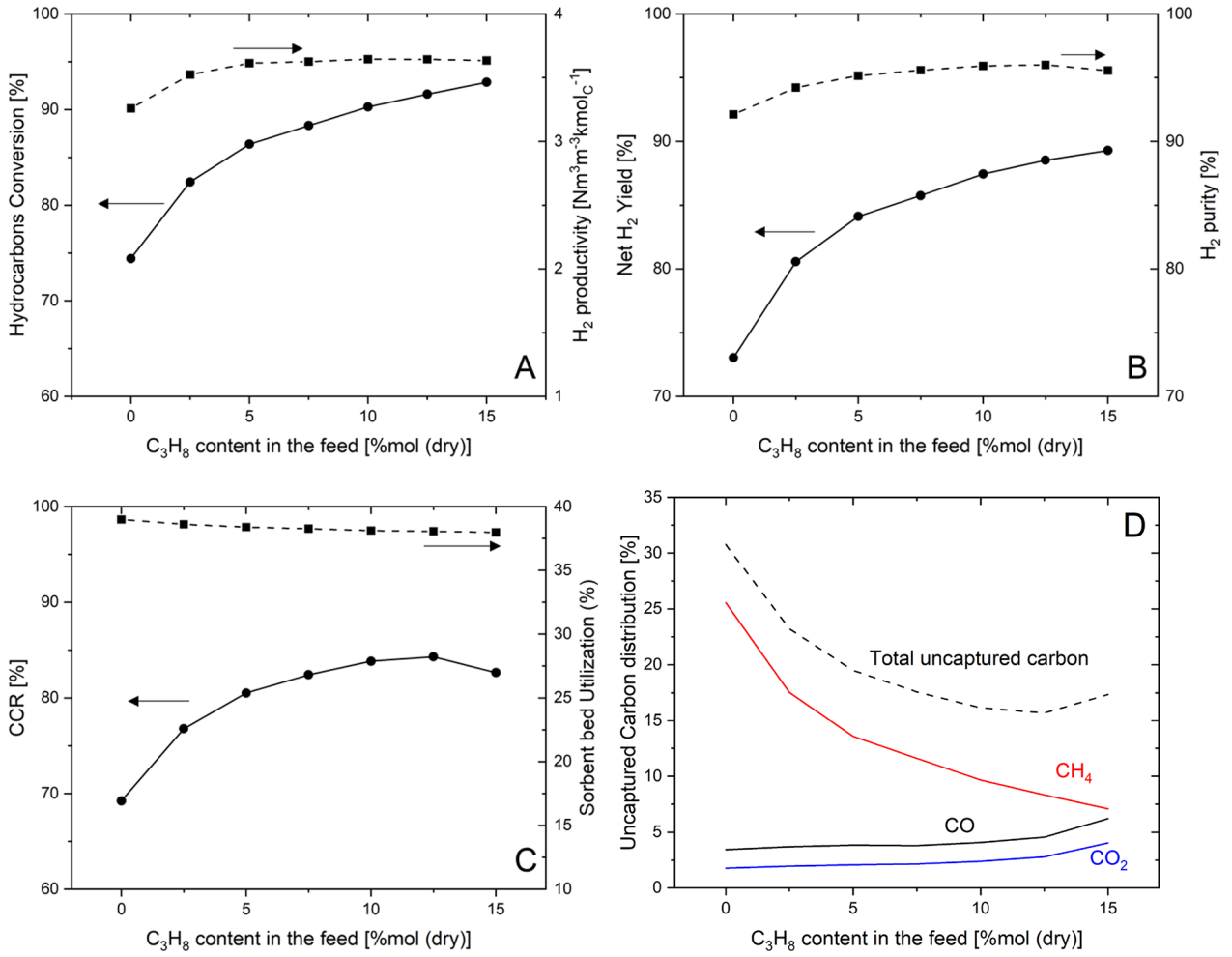

Figure 8. Effect of the C2+ species cofeed on the integral performances of the SER process.

outlet one for most of the reactor's operation duration. Note that at 850 °C, the selected initial solid temperature in the model simulations, equilibrium calculations, as presented in Figure S6, result in almost no carbon capture. These results clearly show that the complex thermal behavior of the adiabatic fixed bed reactor provides a good trade-off between hydrocarbon conversion and carbon capture performances over a wide range of feed stream composition.

CONCLUSIONS

Sorption enhanced reforming of biorefinery side streams for hydrogen production is studied in this work. Using a 1D dynamic heterogeneous model, the effect of the H_2 content in hydrocarbon streams fed to an adiabatic fixed bed reactor is evaluated. Simulations of different H_2 content in the feed are performed and the results show a decrease of 17.1% in the hydrocarbons conversion coupled with a drop of 15.4% of the captured CO_2 on passing from pure CH_4 stream to a feeding stream composed of 40/60 mol/mol H_2/CH_4. The presence of small quantities of C2+ hydrocarbons in the feeding mixture is evaluated as well by assuming a stream containing 40% (dry) hydrogen and 60% (dry) hydrocarbons distributed between propane and methane. Results show an improving trend of the reformer's performance with the increase of the C_3H_8 fraction in the feed, reaching an achievable 92.8% hydrocarbons conversion, while capturing 82.6% of the released CO_2 to produce a stream of 95.6% H_2 purity for a stream composed of 40/45/15 mol/mol $H_2/CH_4/C_3H_8$. The improved performance achieved on the enrichment of H_2/CH_4 mixtures with propane introduces a novel strategy for the feasible SER of complex refinery and biorefinery gaseous side streams.

Comparing the performance indices of a simulated fixed bed reactor with those calculated assuming thermodynamic equilibrium allows a better understanding of the impact of the bed's dynamic thermal behavior. In this case, the presence of a moving carbonation zone, facilitated by the initially high bed temperature (850 °C), leads to a higher simulated integral conversion for pure CH_4, fed at 550 °C, compared to the equilibrium value calculated at 700 °C. However, when H_2 is present in the feed, the simulated integral methane conversion significantly drops, reaching 74.4% for a mixture containing 40% mol H_2, which is much lower than the equilibrium value. The simulations indicate that these limitations can be overcome by increasing the energy stored in the reactor through an increase in the bed heat capacity. For example, using a reactor with an inert heat carrier at a volumetric fraction of 0.34 results in a significant improvement in conversion, reaching 93.4%.

Similarly, in the presence of propane as a model C2+ hydrocarbon, the simulated H_2 yield is higher than the evaluated equilibrium values assessed, which is a result of the moving carbonation zone resulting in the nonuniform temperature profile of the reactor gaining the benefits of

https://doi.org/10.1021/acs.iecr.3c02401
Ind. Eng. Chem. Res. 2023, 62, 15884−15896

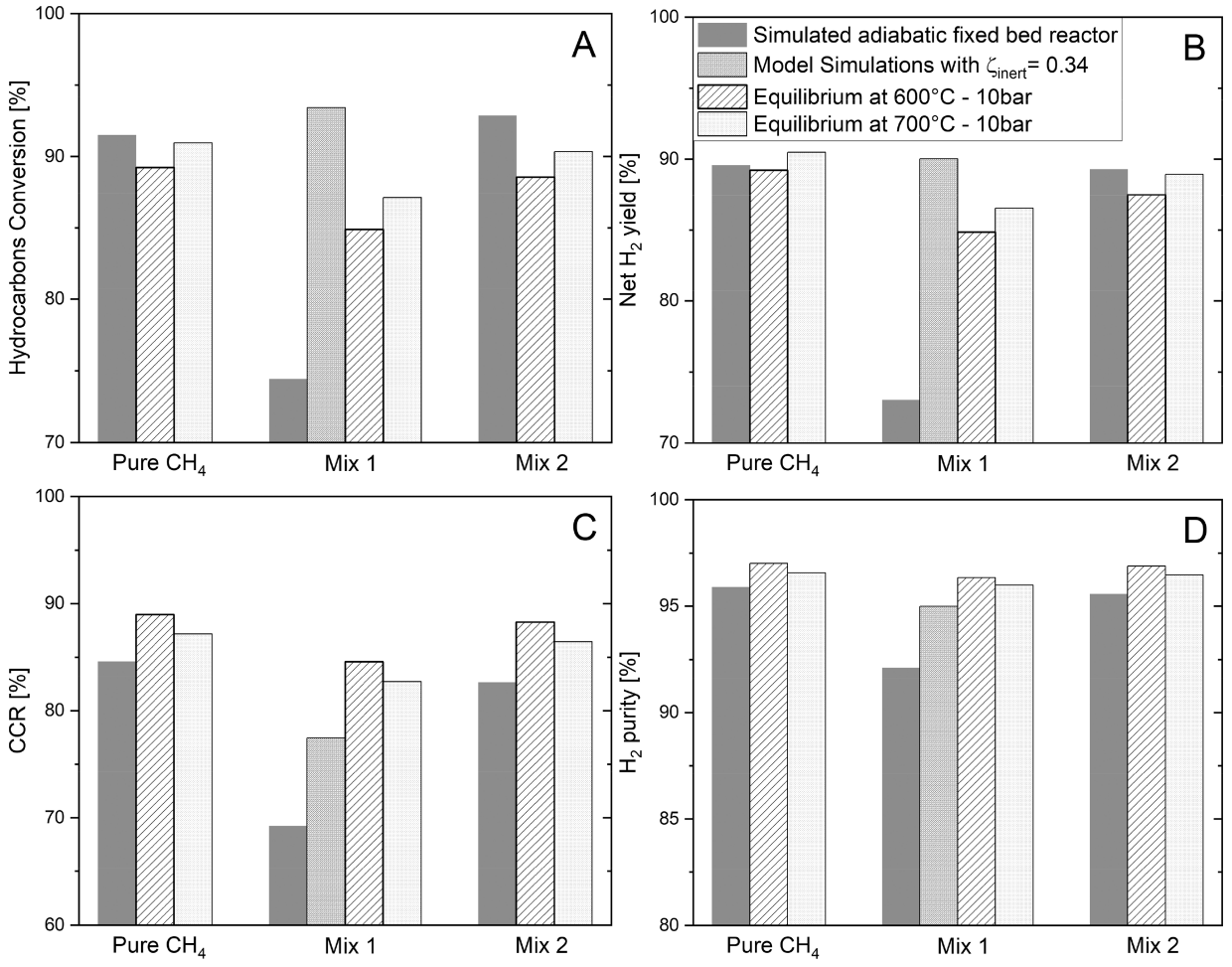

Figure 9. Comparing the performance of the SER of H_2 containing mixtures in a fixed bed adiabatic reactor with equilibrium calculations. Working conditions: P = 10 bar, S/C = 4, Equilibrium at T = 600 °C and T = 700 °C. Model simulations at T_{feed} = 550 °C; $T_{bed,initial}$ = 850 °C.

running the process at high temperature, thus achieving high conversion, while sustaining high CO_2 capture performance.

The results herein presented verifies the technical suitability of using the SER process as a solution for tackling the limits of the conventional steam reforming process regarding the production of H_2 from complex streams that contain high concentration of H_2. With the proper integration between existing industrial plants (refineries, biorefineries, chemical production plants, etc.) and a SER based H_2 production unit utilizing the side streams of the plant, a significant economic advantage may be achieved.

■ ASSOCIATED CONTENT

Supporting Information

The Supporting Information is available free of charge at https://pubs.acs.org/doi/10.1021/acs.iecr.3c02401.

Modeled SER reactor scheme; reactions kinetic scheme of methanation, methane and propane steam reforming, water gas shift, and carbonation reactions used in the simulations; summary of the working conditions for the simulations reported in the work; effect of the steam to carbon ratio and the GHSV on the SER of a H_2-rich stream; thermodynamic analysis; Nomenclature (PDF)

■ AUTHOR INFORMATION

Corresponding Authors

Gianpiero Groppi − *LCCP − Laboratory of Catalysis and Catalytic Processes, Dipartimento di Energia, Politecnico di Milano, 20156 Milano, Italy;* orcid.org/0000-0001-8099-580X; Email: gianpiero.groppi@polimi.it

Alessandra Beretta − *LCCP − Laboratory of Catalysis and Catalytic Processes, Dipartimento di Energia, Politecnico di Milano, 20156 Milano, Italy;* orcid.org/0000-0003-4854-4907; Email: alessandra.beretta@polimi.it

Authors

Abdelrahman Mostafa − *LCCP − Laboratory of Catalysis and Catalytic Processes, Dipartimento di Energia, Politecnico di Milano, 20156 Milano, Italy;* orcid.org/0000-0002-6880-9768

Irene Rapone − *Renewable, New Energies and Material Science Research Center, Eni SpA, 28100 Novara, Italy*

Aldo Bosetti − *Renewable, New Energies and Material Science Research Center, Eni SpA, 28100 Novara, Italy*

Matteo C. Romano − *GECOS − Group of Energy Conversion Systems, Dipartimento di Energia, Politecnico di Milano, 20156 Milano, Italy*

Complete contact information is available at: https://pubs.acs.org/10.1021/acs.iecr.3c02401

https://doi.org/10.1021/acs.iecr.3c02401
Ind. Eng. Chem. Res. 2023, 62, 15884−15896

Author Contributions

The manuscript was written through contributions of all authors. All authors have given approval to the final version of the manuscript.

Notes

The authors declare no competing financial interest.

■ ACKNOWLEDGMENTS

A.M. gratefully acknowledges ENI S.P.A for the financial support under the Ph.D. scholarship agreement with Politecnico di Milano.

■ ABBREVIATIONS

SER, sorption enhanced reforming; SR, steam reforming; WGS, water gas shift; CCR, carbon capture ratio; GHSV, gas hourly space velocity; KPIs, key performance indices; BtT, breakthrough time

■ REFERENCES

(1) International Energy Agency (IEA) World Energy Outlook 2022. https://www.iea.org/reports/world-energy-outlook-2022 (accessed 2023-07−10).

(2) Global Hydrogen Review. https://www.iea.org/reports/global-hydrogen-review-2022 (accessed 2023-07−10).

(3) bp Energy Outlook 2023 edition. https://www.bp.com/en/global/corporate/news-and-insights/press-releases/bp-energy-outlook-2023-explores-key-trends-and-uncertainties-surrounding-the-energy-transition.html (accessed 2023-07−10).

(4) Gomes, J. R. Vegetable Oil Hydroconversion Process. US 2006/0186020 A1, 2006. http://www.google.com/patents/US20060186020.

(5) Jakkula, J.; Niemi, V.; Nikkonen, J.; Purola, V.-M.; Myllyoja, J.; Aalto, P.; Lehtonen, J.; Alopaeus, V. Process for Producing a Hydrocarbon Component of Biological Origin. US 2004/0230085A1, 2004. https://patents.google.com/patent/US20040230085A1/en?oq=US2004%2F0230085A1%2C+2004.

(6) Bosetti, A.; Lombardini, S. F.; Girotti, G. Process for the Production of Olefinic Compounds and a Hydrocarbon Fuel or a Fraction Thereof. US 2016/0251278 A1, 2016. https://patents.google.com/patent/US20160251278A1/en.

(7) Perego, C.; Ricci, M. Diesel Fuel from Biomass. *Catal. Sci. Technol.* **2012**, *2* (9), 1776−1786.

(8) Nurdiawati, A.; Urban, F. Decarbonising the Refinery Sector: A Socio-Technical Analysis of Advanced Biofuels, Green Hydrogen and Carbon Capture and Storage Developments in Sweden. *Energy Res. Soc. Sci.* **2022**, *84*, 102358.

(9) Alves, J. J.; Towler, G. P. Analysis of Refinery Hydrogen Distribution Systems. *Ind. Eng. Chem. Res.* **2002**, *41* (23), 5759−5769.

(10) Gai, L.; Varbanov, P. S.; Van Fan, Y.; Klemeš, J. J.; Nižetić, S. Total Site Hydrogen Integration with Fresh Hydrogen of Multiple Quality and Waste Hydrogen Recovery in Refineries. *Int. J. Hydrogen Energy* **2022**, *47* (24), 12159−12178.

(11) Sikarwar, V. S.; Pfeifer, C.; Ronsse, F.; Pohořelý, M.; Meers, E.; Kaviti, A. K.; Jeremiáš, M. Progress in In-Situ CO2-Sorption for Enhanced Hydrogen Production. *Prog. Energy Combust. Sci.* **2022**, *91*, 101008.

(12) Rodríguez, S.; Capa, A.; García, R.; Chen, D.; Rubiera, F.; Pevida, C.; Gil, M. V. Blends of Bio-Oil/Biogas Model Compounds for High-Purity H2 Production by Sorption Enhanced Steam Reforming (SESR): Experimental Study and Energy Analysis. *Chem. Eng. J.* **2022**, *432*, 134396.

(13) Acha, E.; Chen, D.; Cambra, J. F. Comparison of Novel Olivine Supported Catalysts for High Purity Hydrogen Production by CO2sorption Enhanced Steam Reforming. *J. CO2 Util.* **2020**, *42* (July), 101295.

(14) Gil, M. V.; Rout, K. R.; Chen, D. Production of High Pressure Pure H2 by Pressure Swing Sorption Enhanced Steam Reforming (PS-SESR) of Byproducts in Biorefinery. *Appl. Energy* **2018**, *222* (April), 595−607.

(15) Di Blasi, C.; Signorelli, G.; Di Russo, C.; Rea, G. Product Distribution from Pyrolysis of Wood and Agricultural Residues. *Ind. Eng. Chem. Res.* **1999**, *38* (6), 2216−2224.

(16) Hor, C. J.; Tan, Y. H.; Mubarak, N. M.; Tan, I. S.; Ibrahim, M. L.; Yek, P. N. Y.; Karri, R. R.; Khalid, M. Techno-Economic Assessment of Hydrotreated Vegetable Oil as a Renewable Fuel from Waste Sludge Palm Oil. *Environ. Res.* **2023**, *220*, 115169.

(17) Bezergianni, S.; Kalogianni, A. Hydrocracking of Used Cooking Oil for Biofuels Production. *Bioresour. Technol.* **2009**, *100* (17), 3927−3932.

(18) Bezergianni, S.; Dimitriadis, A.; Kalogianni, A.; Pilavachi, P. A. Hydrotreating of Waste Cooking Oil for Biodiesel Production. Part I: Effect of Temperature on Product Yields and Heteroatom Removal. *Bioresour. Technol.* **2010**, *101* (17), 6651−6656.

(19) Jones, D. S. J., Pujado, R. P., Eds. *Handbook of Petroleum Processing*; Springer, 2004.

(20) Balasubramanian, B.; Lopez Ortiz, A.; Kaytakoglu, S.; Harrison, D.P. Hydrogen from Methane in a Single-Step Process. *Chem. Eng. Sci.* **1999**, *54*, 3543−3552.

(21) Han, C.; Harrison, D. P. Simultaneous Shift Reaction and Carbon Dioxide Separation for the Direct Production of Hydrogen. *Chem. Eng. Sci.* **1994**, *49* (24), 5875−5883.

(22) Iliuta, M. C. CO2 Sorbents for Sorption-Enhanced Steam Reforming. *Adv. Chem. Eng.* **2017**, *51*, 97−205.

(23) Wang, Y.; Memon, M. Z.; Seelro, M. A.; Fu, W.; Gao, Y.; Dong, Y.; Ji, G. A Review of CO2 Sorbents for Promoting Hydrogen Production in the Sorption-Enhanced Steam Reforming Process. *Int. J. Hydrogen Energy* **2021**, *46* (45), 23358−23379.

(24) Antzaras, A. N.; Lemonidou, A. A. Recent Advances on Materials and Processes for Intensified Production of Blue Hydrogen. *Renew. Sustain. Energy Rev.* **2022**, *155*, 111917.

(25) Abanades, J. C.; Alvarez, D. Conversion Limits in the Reaction of CO2 with Lime. *Energy Fuels* **2003**, *17* (2), 308−315.

(26) Di Giuliano, A.; Gallucci, K. Sorption Enhanced Steam Methane Reforming Based on Nickel and Calcium Looping: A Review. *Chem. Eng. Process. - Process Intensif.* **2018**, *130* (May), 240−252.

(27) Harrison, D. P. Sorption-Enhanced Hydrogen Production: A Review. *Ind. Eng. Chem. Res.* **2008**, *47* (17), 6486−6501.

(28) Barelli, L.; Bidini, G.; Gallorini, F.; Servili, S. Hydrogen Production through Sorption-Enhanced Steam Methane Reforming and Membrane Technology: A Review. *Energy* **2008**, *33* (4), 554−570.

(29) Cherbanski, R.; Molga, E. Sorption-Enhanced Steam Methane Reforming (SE-SMR) - A Review: Reactor Types, Catalyst and Sorbent Characterization, Process Modeling. *Chem. Process Eng.* **2018**, *39* (4), 427−448.

(30) Wu, Y. J.; Li, P.; Yu, J. G.; Cunha, A. F.; Rodrigues, A. E. Sorption-Enhanced Steam Reforming of Ethanol for Continuous High-Purity Hydrogen Production: 2D Adsorptive Reactor Dynamics and Process Design. *Chem. Eng. Sci.* **2014**, *118*, 83−93.

(31) Cunha, A. F.; Wu, Y. J.; Santos, J. C.; Rodrigues, A. E. Sorption Enhanced Steam Reforming of Ethanol on Hydrotalcite-like Compounds Impregnated with Active Copper. *Chem. Eng. Res. Des.* **2013**, *91* (3), 581−592.

(32) He, L.; Chen, D. Hydrogen Production from Glucose and Sorbitol by Sorption-Enhanced Steam Reforming: Challenges and Promises. *ChemSusChem* **2012**, *5* (3), 587−595.

(33) Dou, B.; Rickett, G. L.; Dupont, V.; Williams, P. T.; Chen, H.; Ding, Y.; Ghadiri, M. Steam Reforming of Crude Glycerol with in Situ CO2 Sorption. *Bioresour. Technol.* **2010**, *101* (7), 2436−2442.

(34) Fermoso, J.; He, L.; Chen, D. Production of High Purity Hydrogen by Sorption Enhanced Steam Reforming of Crude Glycerol. *Int. J. Hydrogen Energy* **2012**, *37* (19), 14047−14054.

(35) García, R.; Gil, M. V.; Rubiera, F.; Chen, D.; Pevida, C. Renewable Hydrogen Production from Biogas by Sorption Enhanced

https://doi.org/10.1021/acs.iecr.3c02401
Ind. Eng. Chem. Res. 2023, 62, 15884−15896

Steam Reforming (SESR): A Parametric Study. *Energy* **2021**, *218*, 119491.
(36) Mostafa, A.; Rapone, I.; Bosetti, A.; Romano, M. C.; Beretta, A.; Groppi, G. Modelling of Methane Sorption Enhanced Reforming for Blue Hydrogen Production in an Adiabatic Fixed Bed Reactor: Unravelling the Role of the Reactor's Thermal Behavior. *Int. J. Hydrogen Energy* **2023**, *48* (68), 26475−26491.
(37) Xiu, G.; Li, P.; Rodrigues, A. E. Sorption-Enhanced Reaction Process with Reactive Regeneration. *Chem. Eng. Sci.* **2002**, *57* (18), 3893−3908.
(38) Lee, D. K.; Baek, I. H.; Yoon, W. L. Modeling and Simulation for the Methane Steam Reforming Enhanced by in Situ CO2 Removal Utilizing the CaO Carbonation for H2 Production. *Chem. Eng. Sci.* **2004**, *59* (4), 931−942.
(39) Li, Z. S.; Cai, N. S. Modeling of Multiple Cycles for Sorption-Enhanced Steam Methane Reforming and Sorbent Regeneration in Fixed Bed Reactor. *Energy Fuels* **2007**, *21* (5), 2909−2918.
(40) Fernandez, J. R.; Abanades, J. C.; Murillo, R. Modeling of Sorption Enhanced Steam Methane Reforming in an Adiabatic Fixed Bed Reactor. *Chem. Eng. Sci.* **2012**, *84*, 1−11.
(41) Abbas, S. Z.; Dupont, V.; Mahmud, T. Modelling of H2 Production in a Packed Bed Reactor via Sorption Enhanced Steam Methane Reforming Process. *Int. J. Hydrogen Energy* **2017**, *42* (30), 18910−18921.
(42) Xu, J.; Froment, G. F. Methane Steam Reforming, Methanation and Water-gas Shift: I. Intrinsic Kinetics. *AIChE J.* **1989**, *35* (1), 88−96.
(43) Uskov, S. I.; Potemkin, D. I.; Enikeeva, L. V.; Snytnikov, P. V.; Gubaydullin, I. M.; Sobyanin, V. A. Propane Pre-Reforming into Methane-Rich Gas over Ni Catalyst: Experiment and Kinetics Elucidation via Genetic Algorithm. *Energies* **2020**, *13* (13), 3393.
(44) Mess, D.; Sarofim, A. F.; Longwell, J. P. Product Layer Diffusion during the Reaction of Calcium Oxide with Carbon Dioxide. *Energy Fuels* **1999**, *13* (5), 999−1005.
(45) Rodríguez, N.; Alonso, M.; Abanades, J. C. Experimental Investigation of a Circulating Fluidized-Bed Reactor to Capture CO2 with CaO. *AIChE J.* **2011**, *57* (5), 1356−1366.
(46) Mcbride, B.; Gordon, S.; Reno, M. *Coefficients for Calculating Thermodynamic and Transport Properties of Individual Species*; NASA-TM-4513; NASA, 1993.
(47) Pfeffer, R. Heat and Mass Transport in Multiparticle Systems. *Ind. Eng. Chem. Fundam.* **1964**, *3* (4), 380−383.
(48) Wakao, N.; Kaguei, S.; Nagai, H. Effective Diffusion Coefficients for Fluid Species Reacting with First Order Kinetics in Packed Bed Reactors and Discussion on Evaluation of Catalyst Effectiveness Factors. *Chem. Eng. Sci.* **1978**, *33* (2), 183−187.
(49) Poling, B. E.; Prausnitz, J. M.; O'Connell, J. P. *The Properties of Gases and Liquids*, 5th ed.; McGraw-Hill Professional, 2000.
(50) Fuller, E. N.; Ensley, K.; Giddings, J. C. Diffusion of Halogenated Hydrocarbons in Helium. The Effect of Structure on Collision Cross Sections. *J. Phys. Chem.* **1969**, *73* (11), 3679−3685.
(51) Specchia, V.; Baldi, G.; Sicardi, S. Heat Transfer in Packed Bed Reactors with One Phase Flow. *Chem. Eng. Commun.* **1980**, *4* (1−3), 361−380.
(52) Teixeira, P.; Bacariza, C.; Correia, P.; Pinheiro, C. I. C.; Cabrita, I. Hydrogen Production with In Situ CO2 Capture at High and Medium Temperatures Using Solid Sorbents. *Energies* **2022**, *15* (11), 4039.
(53) Fernández, J. R.; Abanades, J. C.; Murillo, R.; Grasa, G. Conceptual Design of a Hydrogen Production Process from Natural Gas with CO 2 Capture Using a Ca-Cu Chemical Loop. *Int. J. Greenh. Gas Control* **2012**, *6*, 126−141.
(54) Fernandez, J. R.; Abanades, J. C.; Grasa, G. Modeling of Sorption Enhanced Steam Methane Reforming-Part II: Simulation within a Novel Ca/Cu Chemical Loop Process for Hydrogen Production. *Chem. Eng. Sci.* **2012**, *84*, 12−20.
(55) Martini, M.; van den Berg, A.; Gallucci, F.; van Sint Annaland, M. Investigation of the Process Operability Windows for Ca-Cu Looping for Hydrogen Production with CO2 Capture. *Chem. Eng. J.* **2016**, *303*, 73−88.

https://doi.org/10.1021/acs.iecr.3c02401
Ind. Eng. Chem. Res. 2023, 62, 15884−15896